Available online at www.sciencedirect.com

ScienceDirect

Procedia Engineering 111 (2015) 220 – 227

Procedia Engineering

www.elsevier.com/locate/procedia

XXIV R-S-P seminar, Theoretical Foundation of Civil Engineering (24RSP) (TFoCE 2015)

Modelling of elastomeric bearings with application of Yeoh hyperelastic material model

Marcin Gajewski[a]*, Radosław Szczerba[b], Stanisław Jemioło[a]

[a]*Warsaw University of Technology, al. Armii Ludowej 16, 00-637 Warsaw, Poland*
[b]*Rzeszów University of Technology, al. Powstańców Warszawy 12, 35-959 Rzeszów, Poland*

Abstract

The application of the hyperelasticity constitutive relationships for modelling of elastomeric bridge bearings is presented. Elastomers which are used for bridge bearings are nearly incompressible materials. Consequently, two models of hyperelasticity for rubber-like materials, i.e. neo-Hookean and Yeoh models are considered. The neo-Hookean model is the simplest possible model of hyperelasticity but unfortunately it has a number of disadvantages (i.e. at certain deformation modes it gives physically unreasonable predictions). The Yeoh model for nonlinear elastic materials is superior to neo-Hookean model and leads to rational description of the behavior of the elastomers for significant elongations and is implemented in many commercial programs using finite element method (FEM). In this work, ABAQUS program is utilized for modelling of chosen bridge bearings. The parameters of two constitutive models are determined based on experimental results and are used in numerical calculations for selected examples of bridge bearings. Concluding remarks are drawn and directions of future research are outlined.

Peer-review under responsibility of organizing committee of the XXIV R-S-P seminar, Theoretical Foundation of Civil Engineering (24RSP)

Keywords: Elastomeric bearings; Hyperelasticity; Yeoh model; Finite element method.

1. Introduction

Elastomeric bearings undergo large strains and deformations that go beyond the limit of applicability of classical theory of small displacements. Consequently, in order to adequately model large displacements and deformations the continuum mechanics has to be applied [1, 2]. For a proper description of elastomer elastic properties the

* Corresponding author. Tel.: +48 22 234 5164; fax: +48 22 825 65 32.
E-mail address: m.gajewski@il.pw.edu.pl

Peer-review under responsibility of organizing committee of the XXIV R-S-P seminar, Theoretical Foundation of Civil Engineering (24RSP)
doi:10.1016/j.proeng.2015.07.080

hyperelasticity theory is used, with a wide range of constitutive models available [3]. In this work, the authors propose a constitutive model that can be reduced to the most well-known hyperelastic material models, i.e. Yeoh, Mooney-Rivlin and neo-Hookean. The main goal of this paper is to present the superiority of the Yeoh model to the most commonly used neo-Hookean model. Although the Yeoh model is not overly complicated it can predict the correct behavior of the elastomer material in uniaxial tension and simple shear tests in the range of a greater extent of deformation than the neo-Hookean or Mooney-Rivlin material models. In the case of neo-Hookean and Yeoh model based on the available in literature experimental tests ([4]) the material parameters for a typical elastomer used for bridge bearings were established. The applicability of the analyzed models is presented through the analysis of the exemplary bridge bearing subjected to compression and shear [5]. For this purpose the finite element method and ABAQUS/Standard software package are applied [6].

2. Constitutive modelling of elastomeric bearings components

2.1. Modelling of steel reinforcements

In the case of bearing steel reinforcing sheets the model of large deformation for elastic-plastic materials was used. This model is a generalization of small deformation plasticity model made by substitution of logarithmic strain tensor in place of small deformation strain tensor in elasticity and plasticity constitutive relationship, cf. [2]. In ABAQUS finite element software it is accessible through the option NLGEOM=ON accompanied by the ELASTIC and PLASTIC constitutive models, cf. [6]. For reinforcing plates the typical steel isotropic elasticity parameters were assumed: E = 210 GPa and $\nu = 0.3$. For ideal plasticity the Huber-Mises yield condition and an associated flow rule were applied with plasticity limit obtained in tension test equal to: $f_y = 235$ [MPa].

2.2. Hyperelasticity models for elastomers

Constitutive model for isotropic incompressible elastomers, which is described in further part of this work, is formulated in the frame of hyperelasticity and proposed in [3]. The fundamental idea of the model is the assumption that stored energy function (SEF) of incompressible rubber-like materials is a regular function with respect to isochoric deformation tensors. As a result in [3] and [5] the following general stored energy function was under investigation:

$$W\left(\bar{I}_1,\bar{I}_2\right)=\frac{1}{2}\Big[a_1\left(\bar{I}_1-3\right)+\frac{1}{2}a_2\left(\bar{I}_1^2-9\right)+\frac{1}{3}a_3\left(\bar{I}_1^3-27\right)+a_4\left(\bar{I}_2-3\right)+a_5\left(\bar{I}_1\bar{I}_2-9\right)\Big]+O\left(\left\|\bar{\mathbf{C}}\right\|^4\right), \tag{1}$$

where a_i are material parameters, and invariants of isochoric deformation tensors can be written in the following form:

$$\bar{I}_1=\mathrm{tr}\bar{\mathbf{B}}=\mathrm{tr}\bar{\mathbf{C}},\quad \bar{I}_2=\mathrm{tr}\bar{\mathbf{B}}^{-1}=\mathrm{tr}\bar{\mathbf{C}}^{-1}. \tag{2}$$

Let us recall that the incompressibility assumption can be written as

$$J-1=\det\mathbf{F}-1=0,\quad \det\mathbf{C}-1=\det\mathbf{B}-1=0, \tag{3}$$

where $\mathbf{F}$ is the deformation gradient tensor, $\mathbf{C}$ and $\mathbf{B}$ are Cauchy-Green right and left stretch tensors ($\mathbf{C}=\mathbf{F}^T\mathbf{F}$, $\mathbf{B}=\mathbf{F}\mathbf{F}^T$, where „T" is a tensor transposition), see [1, 2, 3]. Symbols „tr" and „det" are used respectively as a trace and determinant of the tensor. The deformation tensors and their invariants present in constitutive relationships result from multiplicative decomposition of the gradient tensor $\mathbf{F}$ on volumetric and isochoric parts ($\mathbf{F}=\sqrt[3]{J}\bar{\mathbf{F}}$, $\bar{\mathbf{C}}=\bar{\mathbf{F}}^T\bar{\mathbf{F}}$, $\bar{\mathbf{B}}=\bar{\mathbf{F}}\bar{\mathbf{F}}^T$), cf. [1, 2, 3].

In accordance with the energy conservation law and the incompressibility constraint (3) results, that hyperelasticity constitutive relationship (in Euler description) can be written as:

$$\boldsymbol{\sigma} = -p\mathbf{I} + \bar{\beta}_1\bar{\mathbf{B}} + \bar{\beta}_{-1}\bar{\mathbf{B}}^{-1}, \tag{4}$$

where

$$\bar{\beta}_1 = 2\frac{\partial W}{\partial \bar{I}_1} = a_1 + a_2\bar{I}_1 + a_3\bar{I}_1^2 + a_5\bar{I}_2, \quad \bar{\beta}_{-1} = -2\frac{\partial W}{\partial \bar{I}_2} = -\left(a_4 + a_5\bar{I}_1\right). \tag{5}$$

In general, scalar p can be determined for the given boundary value problem. In (4) $\boldsymbol{\sigma}$ stands for Cauchy stress tensor (sometimes called „true stress tensor"). It should be noted that in order to interpret the results of experimental tests the constitutive relations (4) need to be rewritten in the form with nominal Piola-Kirchhoff stress tensor $\mathbf{S} = J\boldsymbol{\sigma}\mathbf{F}^{-T}$, (see [1, 2, 3])). Already in the early versions of ABAQUS [6] the hyperelasticity model has been implemented in the so-called modified polynomial form proposed by Rivlin in 1948:

$$W = W_D\left(\bar{I}_1, \bar{I}_2\right) + W_I\left(J\right) = \sum_{k+l=1}^{N} C_{kl}\left(\bar{I}_1 - 3\right)^k\left(\bar{I}_2 - 3\right)^l + \sum_{k=1}^{N}\frac{1}{D_k}\left(J-1\right)^{2k}, \tag{6}$$

where, C_{kl} and D_k are material parameters (for $D_k \to 0$ incompressible material model is obtained).

Function (1) is a special case of (6) for parameters a_i expressed as

$$\begin{aligned} &a_1 = 2\left(C_{10} - 3C_{11} - 6C_{20} + 27C_{30}\right), \\ &a_2 = 4\left(C_{20} - 9C_{30}\right), \quad a_3 = 6C_{30}, \quad a_4 = 2\left(C_{01} - 3C_{11}\right), \quad a_5 = 2C_{11}. \end{aligned} \tag{7}$$

The rest of the parameters should be set as equal to zero. Relationships for C_{kl} could be expressed as

$$\begin{aligned} &C_{10} = \frac{1}{2}\left(a_1 + 3a_2 + 9a_3 + 3a_5\right), \\ &C_{20} = \frac{1}{4}\left(a_2 + 6a_3\right), \quad C_{30} = \frac{1}{6}a_3, \quad C_{01} = \frac{1}{2}\left(a_4 + 3a_5\right), \quad C_{11} = \frac{1}{2}a_5. \end{aligned} \tag{8}$$

In [3] it was demonstrated that the model of incompressible material with function (1) leads to a correct evaluation of the influence of invariant $\bar{I}_2$ and its coupling with invariant $\bar{I}_1$.

It was also shown that the SEF (1), with parameters a_i, is more convenient for the analysis of boundary value problem of hyperelastic elastomers than the Mooney-Rivlin proposal (6) used in ABAQUS [6]. It is worth noting that in particular cases of the model according to (1) we can obtain: Yeoh model [7] ($a_4 = a_5 = 0$), Mooney-Rivlin model ($a_2 = a_3 = a_5 = 0$) and neo-Hooken model ($a_2 = a_3 = a_4 = a_5 = 0$).

3. Determination of the hyperelasticity parameters

Material parameters enter linearly to elastomer models proposed in Section 2. Therefore, to determine the parameters of SEF (1) linear optimization method (method of least squares) is applied. It should be emphasized that this is a major advantage of the proposed model (compared to e.g. Ogden models [1] for which nonlinear optimization methods are needed). It means that using linear optimization methods on the basis of experimental results model's parameters can be determined uniquely. To determine the material parameters the simultaneous optimization of the two basic independent experimental tests: uniaxial compression/tension, pure/simple shear was used, cf. [3].

In the case of the incompressible materials the pure shear test is experimentally performed through tension test with plane strain additional assumption, and such test is called planar tension [1, 4]. Explicit form of formulae on the

components of Piola-Kirchhoff stress tensor as a function of elongation (or shear angle) for analyzed experimental tests are given in [5].

The elasticity parameters of elastomer used in the bearings are determined based on the results of experiments published in [4], where among others, the results of uniaxial tension/compression, pure and simple shear tests are included. Several different combinations of experimental data were utilized, which lead to a good approximation of the experimental results with Yeoh model. Some examples of the obtained results were shown in Fig. 1 and Table 1.

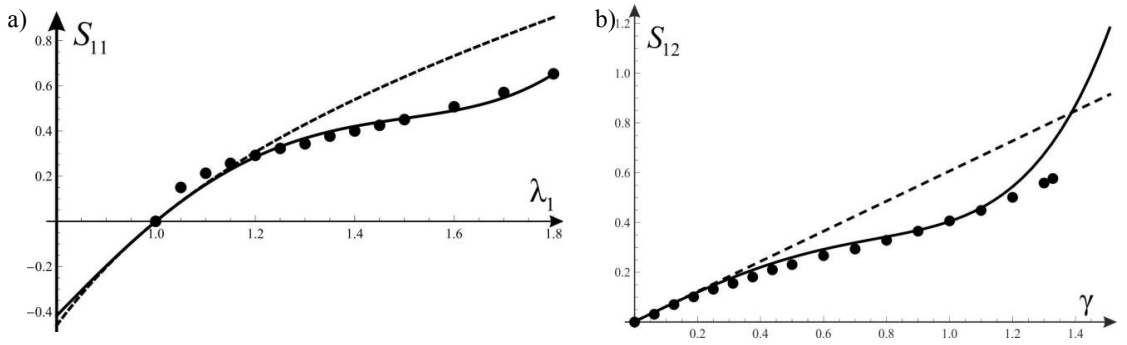

Fig.1. Comparison of the Yeoh (solid line) and neo-Hookean (dashed line) models with experimental data: (a) uniaxial tension; (b) simple shear.

Table 1. Parameters of the Yeoh material model taken under consideration in further analyzes.

Model	C_{10} [*MPa*]	C_{20} [*MPa*]	C_{30} [*MPa*]
MY_1 (parameters obtained on the basis of uniaxial tension and simple shear tests)	0.27337	-0.06226	0.01874
MY_2 (parameters obtained on the basis of uniaxial tension and pure shear tests)	0.30256	-0.10768	0.03778

Based on conclusions presented in [3], in the case of an insufficient number of experimental data (mainly the lack of biaxial test results) the hyperelasticity models, which are independent of the second invariant of isochoric deformations, should be taken into consideration. This remark is confirmed by the analysis of results of the data published in [4].

For the FEM models presented in Section 4 two sets of material parameters contained in Table 1 were adopted. For comparison purposes, neo-Hookean model parameters were assumed on the basis of data presented in Table 1 (in this case the only model parameter is C_{10}). The other simplified models were not analyzed, because they do not lead to satisfactory approximation of the experiments results.

4. Compression and shear tests of elastomeric bridge bearing

4.1. Assumptions of FE models and boundary conditions

In the paper a typical elastomeric bearing, which is commonly used in bridge structures, was taken under consideration. Its geometry and dimensions were shown in Fig. 3. Material parameters were described in previous sections of this work. The considered type of elastomeric bearing was analyzed in three-dimensional space (3D) and also as 2D problem with the plane strain state (PSS) assumption. FEM mesh of the bearing in the plane strain state is illustrated in Fig. 2a. In the case of 2D task the solution convergence analysis was carried out including an influence of the mesh discretization. The mesh was gradually thickening maintaining the size ratios of elements close to the square. Eventually, following mesh using rectangular elements with an approximate length of the element edge was taken under consideration in further analysis: 2.5 [mm] in the case of outer supporting steel plates (8 layers of finite elements on the steel plate thickness), 1.33 [mm] for elastomer (12 layers of finite elements on the elastomer thickness), 1.67 mm [mm] for steel reinforcement sheets (3 layers of finite elements on the steel sheet thickness).

The application of the above described FEM mesh led to a satisfactory convergence of the results with acceptable computation time. Due to the application of hyperelastic models for nearly incompressible materials CPE4RH elements were used that are available in the ABAQUS/Standard library (CPE4RH: 4-node bilinear, reduced integration with hourglass control, hybrid element). FE model in the plane strain state consists of 17520 finite elements and 35355 nodes.

In the case of three-dimensional modelling of the analyzed bearing the symmetry of the bearing geometry and applied load was taken into account. This allows for analyzing of the half-model (including the relevant boundary conditions of symmetry) and significantly reduces the time of numerical calculations. FEM mesh of the bearing in the three-dimensional space is illustrated in Fig. 2b. FEM elements are approximately twice the size of FEM elements taken under consideration for 2D model. C3D8RH elements were used that are available in the ABAQUS/Standard library (C3D8RH: 8-node linear brick, reduced integration with hourglass control, hybrid elements). FE model in the three-dimensional space consists of 120400 finite elements and 249074 nodes.

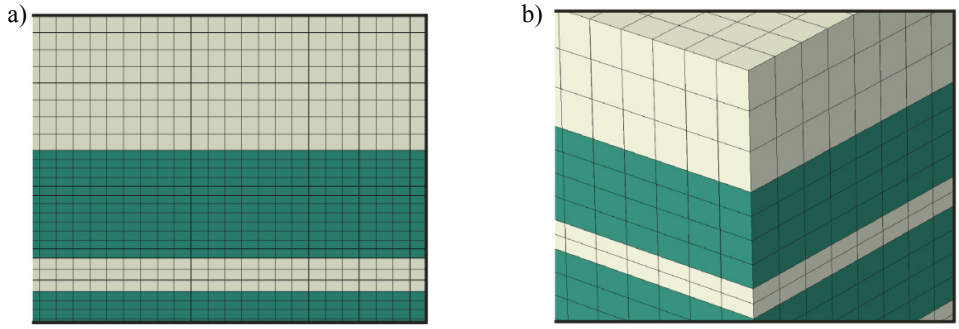

Fig. 2. FEM mesh: (a) in the plane state of strain; (b) in three-dimensional space.

The outer supporting steel plate connected to the bridge span is an element with a very high stiffness. For this reason, the displacement boundary conditions should be applied while performing compression and shearing tests, cf. also results from [5]. For convenience, so-called reference point RP, which is linked to nodes lying on the whole surface of the outer supporting steel plate, was introduced with the use of MPC option available in ABAQUS/Standard. The use of this option leads to the creation of a rigid connection between all the nodes situated on the edge/surface $P_1P_2/P_1P_2P_3P_4$ and reference point RP (see Fig. 3). Total bearing load is applied at reference point RP. At this point it is possible to define both forces (in three directions) and moments (about three axes) or displacements and rotations. All actions are transmitted by the rigid element, so these two types of boundary conditions are equivalent.

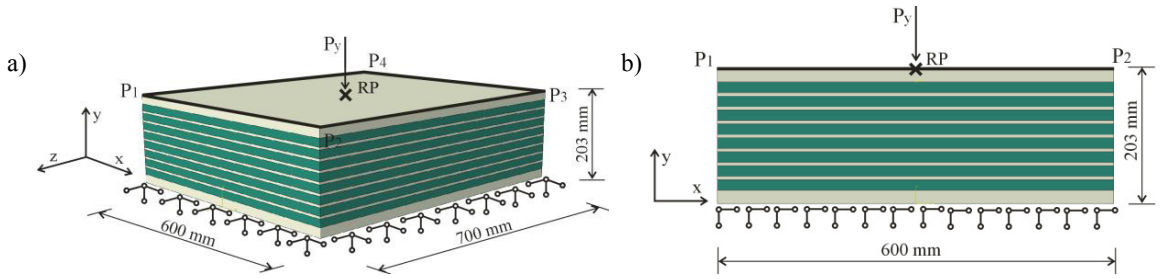

Fig. 3. Boundary conditions applied to outer supporting steel plates with the use of MPC option: (a) 3D FE model; (b) plane strain FE model.

4.2. Compression test

In the case of compression test three constitutive models of hyperelasticity for rubber-like materials were considered: i.e. NH, MY_1 and MY_2. Compression test was carried out by applying a compressive force in the direction of y axis at the reference point RP. Simultaneously, displacements of this node in directions of axes x and z were blocked. The absolute value of the displacement u_y of the reference point RP as a function of bearing compressive force P_y depending on the adopted constitutive model of elastomer was illustrated in Fig. 3. Note that the plane strain theory provides a much greater bearing stiffness than the 3D model (displacement according to PSS are approximately twice lower than in 3D).

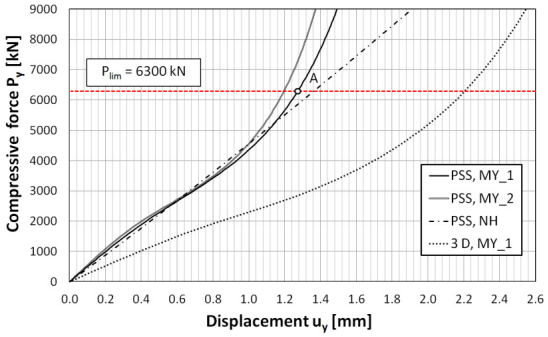

Fig. 4. Bearing compressive force P_y as a function of the displacement u_y of the reference point RP depending on the adopted constitutive model of elastomer. Comparison of compression test results in the case of plane strain and 3D models.

Huber-Mises stress map of elastomeric bearing subjected to compressive force equal to P_y=6300 [kN] (which corresponds to the load capacity of the considered bearing [9]) applied at the reference point RP is presented in Fig. 4. Results are referred to constitutive material model MY_1. It is noteworthy that in this case maximum Huber-Mises stresses reached approximately 77 [MPa] and are located in steel reinforcement sheets in the region of the symmetry axis of the bearing. The maximum stresses in elastomer layers slightly exceeded the value of 3 [MPa]. Additionaly, Fig. 5 presents Huber-Mises stress map of elastomeric bearing obtained for the three-dimensional FE model.

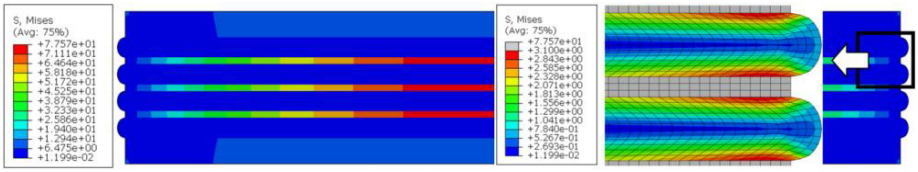

Fig. 5. Huber-Mises stress map of elastomeric bearing in 2D plane strain model subjected to compressive force P_y=6300 [kN] applied at the reference point RP (see point A in Fig. 3).

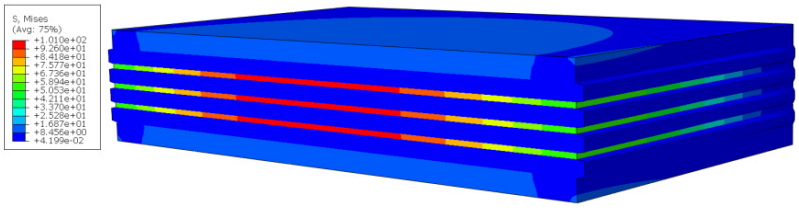

Fig. 6. Huber-Mises stress map of elastomeric bearing 3D model subjected to compressive force P_y=6300 [kN] applied at the reference point RP (MY_1 constitutive model).

4.3. Shear test

In the case of shear test also three constitutive models of hyperelasticity for rubber-like materials were considered: i.e. NH, MY_1 and MY_2. Shear test was carried out by applying the horizontal displacement u_x of the reference point RP (displacement of this node in direction of axis y as well as rotation about z axis were not blocked). The value of the shearing force P_x as a function of horizontal displacement u_x of the reference point RP depending on the adopted constitutive model of elastomer was illustrated in Fig. 6. The graphs clearly show a significant stiffening of bearings in the case of models MY_1 i MY_2 after exceeding the displacement $u_x = 78$ [mm]. The stiffness of the bearing in the case of NH model is at a comparable level in the whole range of displacement. It should also be noted that in the range of displacements specified by the standard (i.e. $u_x < u_{lim}$) regardless of the constitutive models these graphs are nearly the same, see Fig. 6.

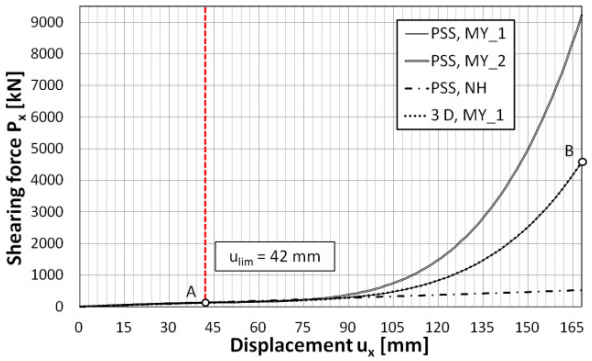

Fig. 7. Bearing shear force P_x as a function of the displacement u_x of the reference point RP depending on the adopted constitutive model of elastomer. Comparison of shear test results in the case of plane strain and 3D models.

Huber-Mises stress maps of elastomeric bearing subjected to horizontal displacement $u_x = 42$ [mm] of the reference point RP (where $u_x = 42$[mm] corresponds to the maximum displacement of the considered bearing allowed by the standard [9]) are presented in Fig. 7. Based on these results, it can be concluded that a fourfold increase of the RP node displacement causes nearly fourfold increase of maximum value of Huber-Misses stresses. A qualitative difference is that the area of stresses close to extreme stresses increased dozen times.

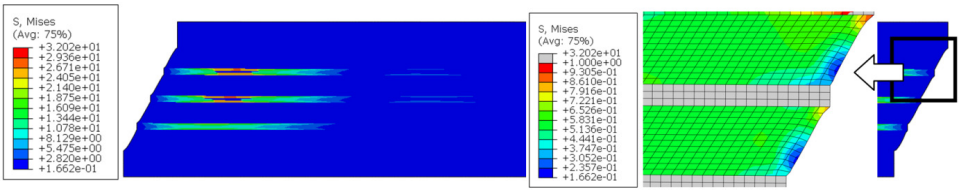

Fig. 8. Huber-Mises stress map of elastomeric bearing plane strain model subjected to displacement u_x of the reference point RP u_x=42 [mm] (see point A in Fig. 6).

Stress map regarding 3D model with the use of MY_1 material model is presented in Fig. 8. Results derived from the use of plane strain and 3D models are very similar (except the areas close to the edges of the bearing). Furthermore, global response of analyzed bearings is nearly the same (curves are overlapping, see Fig 6).

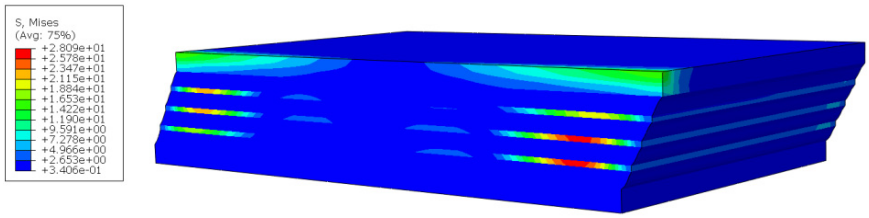

Fig. 9. Huber-Mises stress map of elastomeric bearing for 3D model subjected to displacement u_x=42 [mm] of the reference point RP.

5. Conclusions

- The superiority of the Yeoh hyperelastic material model to neo-Hookean and Mooney-Rivlin models is well visible for the significant values of elongations (shear angle). The Yeoh model for $\lambda_1 > 1.2$ describes properly the behavior of the elastomer in the uniaxial tension/compression tests. Similarly, in the case of simple shear test for $\gamma > 0.2$ the Yeoh model predictions are better than predictions resulting from the use of the neo-Hookean model. These differences, for high displacements values, significantly influence the global response of elastomeric bearings in the case of considered experimental tests, i.e. compression and shear tests. Proper modelling of bearings requires at least the Yeoh model to predict their reasonable behavior for significant deformations that could occur in practice, e.g. when numerically determining the limit load for elastomer bearing.
- For comparison purposes, the discussed elastomer bearing was analyzed as a three-dimensional body as well as a two-dimensional body with plane strain assumption during performing FEM calculations. As far as the global response of considered bearing is concerned, in the case of shear test almost the same results were obtained from 2D and 3D analyzes. In the compression test the differences are significant and global stiffnesses of the bearing do not match from the very beginning. Hence the conclusion that in the case of a complex load histories, in order to avoid significant errors the bearing should be modelled in three-dimensional space.
- For considered elastomer bearing working in the displacement range given in the standard [9] the Huber-Mises equivalent stresses in reinforcing sheets do not exceed 33% of the yield stress in the compression test and 14% of the yield stress in the shear test.
- In the case of application of presented constitutive material model in the dynamic problems (earthquake engineering) it is necessary to take into account also the viscous properties of the material.

References

[1] R.W. Ogden, Non-linear elastic deformations, Ellis Horwood, Chichester, 1984.
[2] S. Jemioło, M. Gajewski, Hipersprężystoplastyczność, Oficyna Wydawnicza PW, Warszawa 2014.
[3] S. Jemioło, Studium hipersprężystych własności materiałów izotropowych, Modelowanie i implementacja numeryczna, Zeszyty Naukowe PW, Budownictwo, z. 140, Warszawa, 2002.
[4] S.L. Burtscher, A. Dorfmann, Compression and shear tests of anisotropic high damping rubber bearings, Engineering Structures, 26, 2004, 1979-1991.
[5] S. Jemioło, M. Gajewski, R. Szczerba, Zastosowanie hipersprężystości i MES w modelowaniu mostowych łożysk elastomerowych, Monografia Sekcji MKiM KILiW PAN.
[6] ABAQUS Theory Manual, ver.6.11, Dassault Systèmes, 2011.
[7] O.H. Yeoh, Some forms of the strain energy function for rubber, Rubber Chemistry and Technology, 66, 1993, 754-771.
[8] J.M. Dulińska, R. Szczerba, Simulation of dynamic behavior of RC bridge with steel laminated elastomeric bearings under high-energy mining tremors, Key Engineering Materials, Trans Tech Publications, Switzerland, Vol. 531–532, 2013, pp. 662-668, doi:10.4028/www.scientific.net/KEM.531-532.662.
[9] PN-EN 1337-1:2003 Structural bearings. General design rules.
[10] A.R. Bhuiyan, Y. Okui, H. Mitamura, T. Imai, A rheology model of high damping rubber bearings for seismic analysis: Identification of nonlinear viscosity, International Journal of Solids and Structures 46, 2009, 1778-1792.
[11] D. Cardone, G. Gesualdi, Experimental evaluation of the mechanical behaviour of elastomeric materials for seismic applications at different air temperatures, International Journal of Mechanical Sciences, 64, 2012, 127-143.
[12] A. Mori, A.J. Carr, N. Cooke, P.J. Moss, Compression behaviour of bridge bearings used for seismic isolation, Engineering Structures, 18 (5), 1996, 351-362.